Intermetallics 89 (2017) 16–21

Contents lists available at ScienceDirect

Intermetallics

journal homepage: www.elsevier.com/locate/intermet

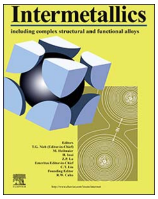

Solubility of Ti in thermoelectric PbTe compound

Genady Komisarchik*, Yaniv Gelbstein, David Fuks

Department of Materials Engineering, Ben-Gurion University of the Negev, Beer-Sheva 84105, Israel

ARTICLE INFO

Keywords:
A. Thermoelectric alloys
B. Density functional theory
C. Heat treatment
E. *Ab initio* calculations
F. Scanning electron microscope
F. X-ray diffraction

ABSTRACT

For the first time, the temperature dependence of the solubility of Ti in PbTe is considered. The potential of Ti doping in PbTe was recently examined both theoretically and experimentally, in which a ~9% efficiency enhancement was observed compared to an undoped PbTe. We present an experimental study of the system for different Ti concentrations indicating the solubility limit of Ti in PbTe and the effect of temperature on the morphology of the alloy. Exceeding the solubility limit leads to phase separation accompanied by formation of the $TiTe_2$ phase. At high temperatures, dissolution of the $TiTe_2$ secondary phase occurs for low Ti concentration, and the system transfers to the single-phase disordered solid solution. On the contrary, for the same temperatures, in the case of higher Ti concentrations the two-phase state is preserved. Theoretical explanation of the observed results is given using *ab inito* calculations combined with the statistical thermodynamic approach. The quasi-binary PbTe-$TiTe_2$ cross-section of the ternary Pb–Ti–Te phase diagram, indicating the Ti solubility in $(Pb_{1-c}Ti_c)Te$ is presented.

1. Introduction

During the last decade, a significant interest is attracted to multi-component compounds for thermoelectric (TE) applications [1]. It is well understood nowadays that alloying of binary or ternary compounds (like lead chalcogenides [2–9] or half-Heusler alloys, HH [10–14]) not only improves the TE properties by controlling the type of charge carriers, shape of the density of states in the vicinity of the Fermi energy, and engineering the band gap, but also allows controlling the morphology of the system for reduction of the lattice thermal conductivity, κ_l [15–19]. The last effect may be achieved by tuning of the fraction of the doping elements. Several mechanisms for controlling of κ_l are usually considered. This reduction may occur in a single-phase state by the scattering of phonons on the atomic length scales through rattling atoms, vacancies, impurities, interstitials, or substitutional atoms (all related to point defects in the material) [5,6]. κ_l can be also decreased by the scattering of phonons by metallic nano-inclusions [11–14,20], by sub-micron phase-separated phases [2,10], or at the interfaces of coherent nanostructures embedded within the matrix [3,21–28]. For the latter, the coherency level of the interfaces between the matrix and a secondary precipitating phase can contribute to the reduction of κ_l and consequently to the *ZT* enhancement [29]. In all of these last examples, phase diagrams are important guiding tools not only for manipulating the phase morphology, but also for understanding the solubility ranges of different doping elements and the relative stability of the phases formed upon the doping. This might significantly enhance the development of new materials [30].

The optimal carrier concentration required for maximizing the TE efficiency is in the scale of $\sim 10^{20}$ carriers/cm^3, as in degenerated semiconductors. In the past decades, the quest for suitable doping candidates of TE compounds such as PbTe continues and especially for donor type materials which usually result in less efficient systems compared to the acceptor type. For a while, Ti was not considered as a suitable dopant for improving the TE properties of PbTe. This is mainly due to the fact that although forming resonant levels in the bottom of the conduction band (Ti is an electron donor in PbTe), it did not contribute to the carrier concentration and did not increase the thermopower compared to other classical *n*-type impurities [32–34]. Although experimental attempts to link the Ti doping level of PbTe with the TE properties were made [33,35], experimental research on the thermodynamic properties and phase stability of the $(Pb_{1-c}Ti_c)Te$ ternary system is scarce and further studies are needed. Even for the binary Pb–Ti system, the solubility limit of Ti in Pb is unknown due to the very small atomic fraction of Ti that may be dissolved in Pb forming a dilute solid solution. A recent experiment, focused on the TE potential of the system, made two important observations [31]. First, a solubility limit of about 0.5 at% Ti in the Pb sub-lattice of PbTe was identified. Beyond this composition, precipitation of the $TiTe_2$ phase occurred. The second observation which is displayed in Fig. 1, showed that a low Ti concentration of ~0.1 at% led to optimal TE properties with a remarkable figure of merit, *ZT*, of ~1.2 at 500 °C, while for higher Ti atomic fractions of ~1–3 at% the *ZT* was significantly decreased. The

---

* Corresponding author.
E-mail address: genadyk@post.bgu.ac.il (G. Komisarchik).

http://dx.doi.org/10.1016/j.intermet.2017.05.016
Received 20 April 2017; Received in revised form 14 May 2017; Accepted 22 May 2017

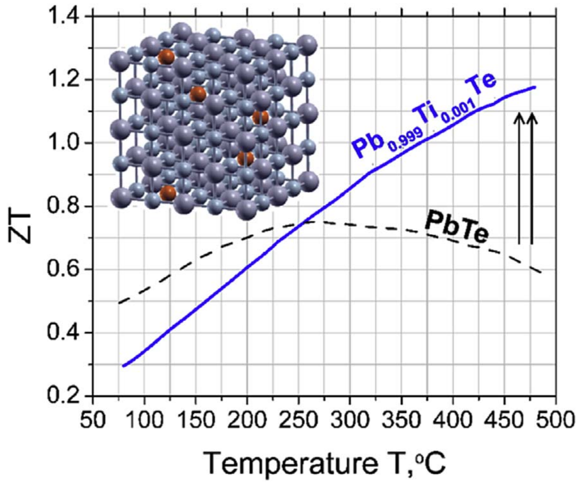

Fig. 1. The enchantment of the figure of merit, *ZT*, in the ($Pb_{1\text{-}c}Ti_c$)Te system. Adding Ti to PbTe in lower concentrations than the solubility limit enhances the efficiency values at high temperatures [31]. A schematic structure illustrating the disordered distribution of Ti atoms in the Pb sub-lattice is inserted in the figure. Gray, turquoise and orange balls correspond to Pb, Te, and Ti atoms, respectively. (For interpretation of the references to colour in this figure legend, the reader is referred to the web version of this article.)

variation in the unit cell parameters between PbTe ($a_O = 6.561$ Å) and $TiTe_2$ ($a_O = 3.78$ Å, $c_O = 6.50$ Å) [36] suggest a sufficient mismatch in the interface, contributing to the κ_l reduction observed experimentally for Ti concentrations slightly above the solubility limit. Recently, the solubility limit of Ti in the Pb sub-lattice was shown to be lower at room temperature but no temperature dependent values were provided [37]. In this context, the information about the temperature dependent solubility of Ti in PbTe is necessary for both electronically optimization of the carrier concentration toward the $\sim 10^{20}$ carriers/cm^3 range and controlling the morphology and the stability of the secondary $TiTe_2$ phase for minimizing of κ_l. In this paper, we experimentally analyze dilute ($Pb_{1\text{-}c}Ti_c$)Te solid solutions forming a single phase state at high temperatures and theoretically estimate the temperature dependent solubility limit of Ti. Density functional theory (DFT) study combined with the statistical thermodynamics approach is applied to analyze the solubility of Ti in the Pb sub-lattice immersed in the background of the rest Te atoms. In contradiction to a previous application [12] of DFT calculations combined with the concentration wave (CW) approach [38] to analyze phase stability beyond $T = 0$ K, here we present a much less time and computational effort consuming way to estimate the solubility of Ti in PbTe that allows explanation of the obtained experimental results.

2. Methodology

2.1. Experimental

Samples with the ($Pb_{0.995}Ti_{0.005}$)Te and ($Pb_{0.97}Ti_{0.03}$)Te compositions were prepared in the method described previously in Ref. [31]. Synthesizing the samples by arc-melting followed by heat treatment and hot pressing, was found to be optimal for obtaining dense ($>$ 95% of the theoretical density) and homogeneous samples. Following the described preparation method, each of the investigated compositions was additionally thermal treated. For this purpose, the samples were sealed in evacuated quartz ampoules under vacuum of 10^{-6} Torr and subsequently placed in a rocking furnace (Thermcraft inc.) for 7 days at 1073 K, then quenched in ice water. The crystal structures of the samples were analyzed by x-ray powder diffraction (XRD; Rigaku DMAX 2100 powder diffractometer). The microstructural characterizations and the chemical composition analysis were conducted by high resolution scanning electron microscopy (HRSEM; JEOL JSM-7400) and energy-dispersive X-ray spectroscopy (EDS), respectively.

Table 1
Comparison of the calculated properties of PbTe with the results of previous publications. m_O is the mass of free electron. L, W and Γ are high symmetry points of the Brillouin zone (BZ) for rock-salt structure.

Property	Current work	Previous studies
Lattice parameter, a (Å)	6.561	6.561 [42], 6.454 [43] 6.462 [44]
Bulk modulus, B (GPa)	41.1	38.9 [45]
Energy gap, E_g (eV)	0.24	0.19 [46–48], 0.22 [49], 0.29–0.32 [50]
Transversal effective mass, L → W direction in BZ, m_T^*	$0.017m_O$	$0.016m_O$ [51]
Longitudinal effective mass, L → Γ direction in BZ, m_L^*	$0.165m_O$	$0.151m_O$ [51] $0.195m_O$ [52]
Concentration of holes, (cm^{-3})	$3.15 \cdot 10^{18}$	$3.0 \cdot 10^{18}$ [53]
Sound velocity, V_s (10^5 cm/s)	1.928[a]	1.452 [54]
Debye temperature, θ_D (K)	220.5[a]	176.7 [54]

[a] For polycrystalline PbTe based on the approach described in Ref. [55].

2.2. Theory

2.2.1. Computational details

DFT using the Full Potential method with the Linearized Augmented Plane Waves (FP-LAPW) formalism, as implemented in the WIEN2k code (Version 10.1) [39–41] was applied in all of the calculations. The applied parameters required for the calculations were previously described in Ref. [37]. As can be definitely seen from Table 1, the calculated results are in a good agreement with previously reported experimental and/or calculated data.

It is noteworthy that the electronic properties of this *p*-type material, including the energy gap and effective masses of holes calculated from the energy spectra, agree well with previously reported results. Also, the concentration of holes obtained for $T = 80$ K by integrating the total density of states with the Fermi-Dirac function is in a good agreement with measurements at $T = 77$ K for monocrystals of PbTe [53].

2.2.2. Thermodynamic route

In the current study of the solubility range of Ti in PbTe, *ab initio* DFT calculations were combined with a statistical thermodynamic approach. This method was thoroughly described in Ref. [37]. In ($Pb_{1\text{-}c}Ti_c$)Te solid solutions, Ti substitute Pb atoms. This allows to consider a face centered cubic (FCC) Pb/Ti sub-lattice in a rock-salt ($Pb_{1\text{-}c}Ti_c$)Te structure as immersed in the field of the rest Te atoms that occupy the same positions as in pure PbTe. In this paper, this approach is applied for studying the decomposition in the Pb/Ti sub-lattice at different temperatures. The variation in the atomic fraction of Ti changes the charge distribution as accounted in the *ab initio* calculations. These calculations are self-consistent. It means that the redistribution of the electron charge, in the different phases investigated in the study, is accounted during calculations to run to convergence. Simultaneously, the potential background formed by the Te atoms is changing when different superstructures in the Pb/Ti sub-lattice (even with the same atomic fraction of constituents) are considered. Due to the self-consistent character of the calculations, the charge transfer that determines the Ti bonding with the surrounding atoms is also automatically accounted and changes, as follows from the meaning of the self-consistent study. The idea of considering one of the sub-lattices as immersed in the field of the rest of the lattice was successfully applied in thermodynamic analyses of ceramic crystals [56], to describe the spinodal decomposition in (Ti,Al)N solid solutions [57–59], to explain the behavior of complex perovskites [60–63], and to analyze the initial stages of the growth of thin metallic films on a ceramic substrate [64–66]. Furthermore, it was applied for the description of the phase competition in $TiNiSn–TiNi_2Sn$ [12] and in predictions of phase competition in the USi_3-UAl_3 phase diagram [67]. It was also explored